

## Article

# Bayesian Regularization Neural Network-Based Machine Learning Approach on Optimization of CRDI-Split Injection with Waste Cooking Oil Biodiesel to Improve Diesel Engine Performance

Babu Dharmalingam <sup>1</sup>, Santhoshkumar Annamalai <sup>2</sup> , Sukunya Areeya <sup>1</sup>, Kittipong Rattanaporn <sup>3</sup> , Keerthi Katam <sup>4</sup>, Pau-Loke Show <sup>5,6,7,8</sup>  and Malinee Sririyanun <sup>1,\*</sup> 

<sup>1</sup> Biorefinery and Process Automation Engineering Center, Department of Chemical and Process Engineering, TGGS, King Mongkut's University of Technology North Bangkok, Bangkok 10800, Thailand

<sup>2</sup> Mechanical Engineering, Kongu Engineering College, Perundurai 638060, India

<sup>3</sup> Department of Biotechnology, Faculty of Agro-Industry, Kasetsart University, Bangkok 10900, Thailand

<sup>4</sup> Department of Civil Engineering, Ecole Centrale School of Engineering, Mahindra University, Telangana 500043, India

<sup>5</sup> Department of Chemical Engineering, Khalifa University, Shakhboub Bin Sultan St. Zone 1, Abu Dhabi P.O. Box. 127788, United Arab Emirates

<sup>6</sup> Zhejiang Provincial Key Laboratory for Subtropical Water Environment and Marine Biological Resources Protection, Wenzhou University, Wenzhou 325035, China

<sup>7</sup> Department of Sustainable Engineering, Saveetha School of Engineering, SIMATS, Chennai 602105, India

<sup>8</sup> Department of Chemical and Environmental Engineering, Faculty of Engineering, University of Nottingham Malaysia, Semenyih 43500, Malaysia

\* Correspondence: macintous@gmail.com



**Citation:** Dharmalingam, B.; Annamalai, S.; Areeya, S.; Rattanaporn, K.; Katam, K.; Show, P.-L.; Sririyanun, M. Bayesian Regularization Neural Network-Based Machine Learning Approach on Optimization of CRDI-Split Injection with Waste Cooking Oil Biodiesel to Improve Diesel Engine Performance. *Energies* **2023**, *16*, 2805. <https://doi.org/10.3390/en16062805>

Academic Editor: Attilio Converti

Received: 14 February 2023

Revised: 13 March 2023

Accepted: 14 March 2023

Published: 17 March 2023



**Copyright:** © 2023 by the authors. Licensee MDPI, Basel, Switzerland. This article is an open access article distributed under the terms and conditions of the Creative Commons Attribution (CC BY) license (<https://creativecommons.org/licenses/by/4.0/>).

**Abstract:** The present study utilized response surface methodology (RSM) and Bayesian neural network (BNN) to predict the characteristics of a diesel engine powered by a blend of biodiesel and diesel fuel. The biodiesel was produced from waste cooking oil using a biocatalyst synthesized from vegetable waste through the wet impregnation technique. A multilevel central composite design was utilized to predict engine characteristics, including brake thermal efficiency (BTE), nitric oxide (NO), unburned hydrocarbons (UBHC), smoke emissions, heat release rate (HRR), and cylinder peak pressure (CGPP). BNN and the logistic-sigmoid activation function were used to train the experimental data in the artificial neural network (ANN) model, and the errors and correlations of the predicted models were calculated. The study revealed that the biocatalyst was capable of producing a maximum yield of 93% at 55 °C under specific reaction conditions, namely a reaction time of 120 min, a stirrer speed of 900 rpm, a catalyst loading of 7 wt.%, and a molar ratio of 1:9. Further, the ANN model was found to exhibit comparably lower prediction errors (0.001–0.0024), lower MAPE errors (3.14–4.6%), and a strong correlation (0.984–0.998) compared to the RSM model. B100-80%-20% was discovered to be the best formulation for emission property, while B100-90%-10% was the best mix for engine performance and combustion at 100% load. In conclusion, this study found that utilizing the synthesized biocatalyst led to attaining a maximum biodiesel yield. Furthermore, the study recommends using ANN and RSM techniques for accurately predicting the characteristics of a diesel engine.

**Keywords:** central composite design; Bayesian regularization neural network; split injection strategy; mixed waste cooking oil methyl ester; common rail direct injection diesel engine

## 1. Introduction

The depletion of fossil fuels results from population growth, industrialization, and technological advancements. Burning these fuels in diesel engines results in the emission of harmful pollutants that contribute to various environmental problems, such as ozone

depletion, global warming, climate change, and pollution of the environment [1]. Hence, environmental organizations like the EPA have forced people in business and scientific areas to search for renewable sources for sustaining market growth [2]. Biodiesel has received much attention as an environmentally beneficial substitute for petroleum diesel due to several positive characteristics, such as being biodegradable, renewable, nontoxic, having good emissions properties, no sulfur, and good miscibility with diesel [3]. The traditional edible feedstock is discouraged due to land constraints and creating the conflict between food and fuel. Therefore, the primary focus is cost-effective alternatives to traditional oil sources, including animal fats, waste cooking oil, and algae oil [4]. Owing to its low cost and wide availability, waste cooking oil is one of the preferred feedstock used in biodiesel production, alongside other feedstock. This type of oil can be obtained by collecting and processing used edible oil, typically from food frying. In Bangkok, Thailand, major hotels, hostels, restaurants, and homes generate a considerable amount of waste cooking oil annually. Unfortunately, poor waste management systems in the area have led to environmental pollution issues associated with the disposal of waste cooking oil [5]. Therefore, effectively utilizing WCO in biodiesel production is the only viable solution for waste management.

The recovery of homogeneous catalysts can be difficult, making it challenging to reuse them in biodiesel production. Additionally, using such catalysts can result in soap formation during transesterification, leading to lower biodiesel yields. As a result, extra purification and separation steps may be necessary [6]. In contrast, heterogeneous catalysts are receiving more attention as a superior alternative because of their high thermal stability, non-toxicity, noncorrosivity, ecologically acceptability, and reusability. Moreover, the cost of making biodiesel could be decreased by synthesizing heterogeneous catalysts from waste products [7]. A modification process was conducted on zeolite using barium to enhance its catalytic activity for biodiesel production from used frying oil. This process involved a coprecipitation technique, followed by thermal treatment, resulting in improved biodiesel properties. The modified zeolite showed potential as a viable alternative to traditional biodiesel production methods [8].

Biodiesel is considered an alternative fuel for diesel engines owing to its desirable fuel properties. However, its high viscosity and bulk modulus can negatively affect engine combustion efficiency and increase the risk of injector damage. Additionally, the larger droplets in biodiesel may hinder atomization, leading to reduced engine performance [9]. In recent years, modern engine technology has adopted an advanced injection strategy to enhance performance and reduce NO and smoke emissions [10]. On the other hand, operating conditions were optimized in a CRDI engine running on a blend of palm oil (20%) and neat diesel (80%) to minimize NO emissions. The optimization involved using a pilot injection of 10% and a higher pressure than a single injection. This resulted in a 40% reduction in NO emissions and a reduction in smoke, UBHC, and CO emissions by 26.2%, 19.2%, and 21.5%, respectively. These findings suggest that optimizing engine operating conditions can effectively reduce emissions in biodiesel-blended fuels [11]. Likewise, multi-objective optimization was applied to operate the CRDI-assisted diesel engine fueled with Sapota biodiesel. The study revealed that the in-cylinder pressure and HRR were found to be maximum when using Sapota biodiesel blends at CR of 19 and 0% EGR, and the NO emission was 61% less than the diesel operation when 19 and 0% EGR blends at CR were tested [12]. Moreover, the CRDI-assisted diesel engine fueled with waste cooking oil biodiesel utilized a combination of split injection and RCCI dual-fuel combustion. The results of NO emissions were lowered from 8.1 to 6.5 g/kWh under the optimal split injection condition, and the smoke emission in RCCI-dual mode decreased from 46% to 19% [13]. The RSM-based central composite design was used to optimize the diesel engine performance, emission, and combustion characteristics. The study reported that the RSM predicted values were good agreement with the experimental results [14]. Alternatively, an artificial neural network (ANN) was employed to optimize biodiesel production from Aegle marmelose Correa seeds. The results indicated that the LMNN method demon-

strated a higher level of accuracy in predicting yield, with a superior  $R^2$  value. These findings underscore the potential benefits of employing ANN techniques in optimizing biodiesel production processes [15]. Another study employed three different methods to optimize the parameters in biomass pretreatment, including the BRNN, SCGNN, and LMNN network [16]. The study reported that the BRNN model was found to be a more accurate prediction compared to other methods with better  $R^2$  values and lower MSE. Tosun et al. [17] used an ANN approach to forecast the engine characteristics fueled with peanut methyl ester with alcohol. The study utilized the logistic sigmoid as an activation function in the hidden layer and the linear transfer function in the output layer to develop an ANN model. The results demonstrated the superiority of the ANN model compared to linear regression, as indicated by lower MAPE values [17]. The results emphasize the importance of utilizing bio-based heterogeneous catalysts to produce biodiesel from waste cooking oil.

The primary objective of this study is to produce biodiesel from waste cooking oil utilizing a bio-based catalyst synthesized from vegetable wastes via the calcination method. The catalyst was also characterized using XRD to determine its properties. Additionally, a statistical analysis was conducted using a central composite design-based RSM model to improve and optimize biodiesel production. Further, the impact of process parameters, including temperature, molar ratio, catalyst loading, reaction time, and stirrer speed on biodiesel production were investigated. Most of the research has studied the behavior of diesel engine combustion and emission characteristics under standard operating conditions; not enough study has been done to develop specifically at full load operation and different injection timing and higher injection pressure. To increase fuel efficiency and reduce emissions, this study searches for the best injection technique based on the use of a split injection strategy. Split injection refers to a fuel injection process in which the fuel is injected at different timing and quantities, and it also controls the injection duration. The primary objective of this investigation is to examine the combustion and emission traits of a CRDI-assisted diesel engine utilizing diesel and biodiesel, subject to split injection policy by altering the injection timing and quantity. In addition, the optimization and prognosis of diesel engine traits fueled with biodiesel and diesel are carried out using RSM and ANN techniques.

## 2. Materials and Methods

### 2.1. Bio-Catalyst Synthesis from Vegetable Wastes

Vegetable wastes, including Chinese broccoli, Napa cabbage and cauliflower, were procured from a local market located in Bangkok, Thailand. Additionally, ethanol was purchased from Sigma Aldrich, Thailand. The incipient wet impregnation method was employed to produce bio-catalyst from vegetable wastes. The collected samples were manually cut into slices with a 1 cm diameter. The dried samples were subsequently filtered and sieved through an aluminum mesh before being subjected to heat treatment at 110 °C for 24 h in a hot-air oven to remove moisture. Vegetable waste was crushed into a powder form. The powder was converted into carbon using HCl by the wet impregnation method. The acid-activated carbon had a pH value around 2–3. Water washing needed to be carried out in order to reduce the acid value in the range of 6–7. The neutralized carbon was used as catalyst support for biodiesel production. The purpose of acid activation is to reduce the calcination temperature and increase the surface area of the carbon support. It is supposed to be performed before the calcination process. Thus in turn, it reduced the energy required for the calcination and improved the surface area. Calcination was then performed in a nitrogen environment at 800 °C for 3 h, which was determined to be the optimal temperature as the surface area did not significantly change beyond this point. The resulting calcined sample was washed with distilled water until the pH reached 6–7, after which it was cleaned with water and subjected to another round of heat treatment at 110 °C for 12 h to synthesize the bio-based catalyst from vegetable wastes. These procedures were meticulously carried out to ensure the highest quality and purity of the final product.

## 2.2. Biodiesel Synthesis

Sunflower and palm oil were procured from a local market located in Bangkok, Thailand. To purify the mixed waste cooking oil (MWCO), water and food solids particles were removed using a centrifuge for 2 h at 5000 rpm. Furthermore, 100 g of MWCO was heated at 80 °C for 30 min before being transferred to the separating funnel. The prepared MWCO was rinsed with distilled water to remove any lingering water and smell being heated at 110 °C. The acid value of MWCO was found to be 3.4 mg KOH/g, which is higher than the required value of less than 1 mg KOH/g for transesterification. Therefore, an esterification process was carried out on MWCO under specific conditions such as 55 °C temperature, stirrer speed of 900 rpm, 1% phosphoric acid, 90 min of reaction time, and a 1:3 molar ratio. As a result, the acid value of MWCO was reduced to 1 mg KOH/g. The transesterification process was carried out in a 200 mL round bottom flask equipped with a heating mantle, thermocouple, condenser, and magnetic stirrer. Initially, 100 g of waste cooking oil, methanol, and bio-catalyst were thoroughly mixed in a conical flask before being fed into the reactor. Following that, the mixture was agitated for the allotted reaction time as per the experimental matrix. Following the reaction, the product was given 24 h to settle in a gravity separating funnel, and solid catalyst was settled at the bottom phase (Figure 1). The biodiesel was settled on the top layer of the glycerol, which had dropped the funnel's bottom side. Afterward, the raw biodiesel was cleaned with distilled water and separated in a separating funnel and heated at 110 °C to remove the moisture content.

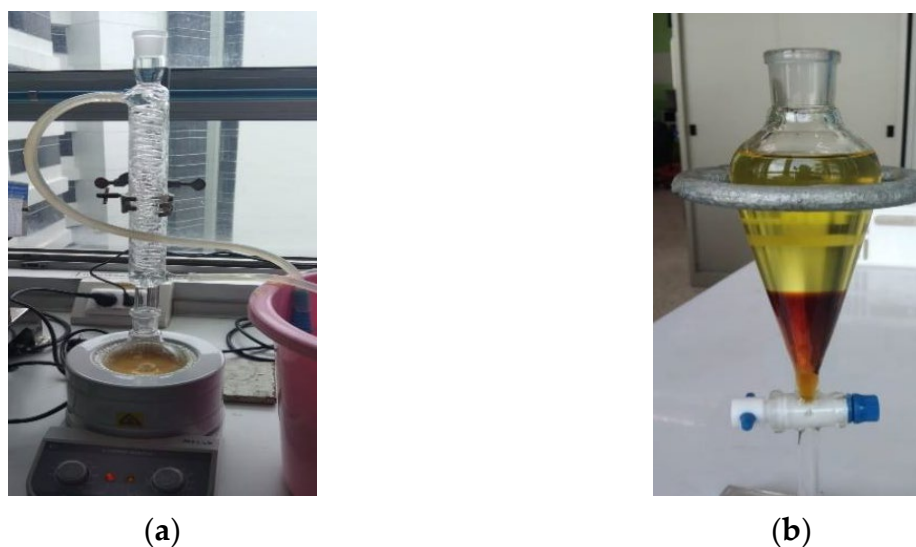


**Figure 1.** Photographic view of the (a) biodiesel setup and (b) purified biodiesel in the top layer.

## 2.3. Optimization of Diesel Engine Performance, Emissions, and Combustion Characteristics Using Response Surface Methodology

The three experimental design methodologies, Response Surface Methodology, Taguchi Method, and Factorial Design, can be widely applied in engineering domains to optimize process parameters. These methodologies find use in various sectors such as petroleum refining, food engineering, biodiesel production, and optimizing diesel engine performance, emissions, and combustion characteristics [16]. Mainly, RSM is used to model nonlinear relationships between input and output results, factorial design is used to model linear relationships, and the Taguchi technique identifies the best set of factors [18]. In this work, the process parameters for the production of biodiesel were optimized using response surface methodology based on a central composite design approach. The study also wanted to determine the combustion and emission characteristics of a CRDI-assisted diesel engine fueled with mixed waste cooking oil biodiesel and diesel blends. The point prediction method was applied to optimize biodiesel production and engine characteristics. The experimental study made use of a design matrix, as shown in Table 1, in which the biodiesel

yield ( $Y$ , %) was the output response and the input parameters were time ( $X_1$ , 30–150 min), temperature ( $X_2$ , 45–65 °C), catalyst loading ( $X_3$ , 1–9 wt.%), molar ratio ( $X_4$ , 1:3–1:15), and stirrer speed ( $X_5$ , 300–1500 rpm). Similarly, main injection timing ( $X_1$ , 17–25 °C), post-injection timing ( $X_2$ , 7 °C bTDC–7 °C aTDC), main injection quantity ( $X_3$ , 70–90%), post-injection fuel quantity ( $X_4$ , 10–30%), and fuel proportion ( $X_5$ , diesel and biodiesel) were designated as input variables and BTE, CO, UBHC, NO, smoke, CGPP, and HRR were output responses. The input variables and the combination for the experimental study are illustrated in Table 2. Post-injection timing is crucial in diesel engine control, affecting performance, emissions, and fuel efficiency. Injecting fuel after the main injection event can reduce engine noise, particulate matter, and nitrogen oxide emissions while improving fuel efficiency. Proper calibration is essential to optimize engine performance and meet regulatory standards.

**Table 1.** Experimental matrix for transesterification reaction at various conditions.

Molar Ratio (% $v/v$ )	Catalyst (%wt.)	Temperature (°C)	Time (Min)	Speed (rpm)	FAME Yield (%)
9	7	60	120	600	90
3	5	65	150	300	75
9	7	60	120	900	93
6	9	50	60	600	82
9	7	55	90	600	91
3	5	45	30	300	75
9	9	60	60	600	90
12	3	65	120	300	82
3	1	55	30	1500	73
12	7	45	120	1200	76
9	7	55	60	600	91
15	3	65	30	1200	75
12	7	45	90	1500	80
6	5	60	90	900	90
12	3	65	150	300	82
6	7	55	60	900	89
3	1	45	90	1200	73
6	5	50	90	900	86
12	1	45	150	1500	73
6	9	50	120	600	89
9	7	60	30	600	91
6	3	50	90	900	83
15	5	50	60	600	81
3	9	65	150	1200	76
3	1	45	150	300	72
15	9	60	60	900	86
15	5	50	90	600	81
3	3	45	120	1200	73
12	5	50	30	300	75
15	7	50	120	900	84
12	1	55	150	1500	73
3	9	65	120	300	81

**Table 2.** The input variables and the combination for the experimental study of engine characterization.

Main Injection Timing (°C)	Post-Injection Timing (°C)	Main Injection Quantity (%)	Post-Injection Quantity (%)	Fuel Proportion
19	−7	80	20	B80-20
23	−7	90	10	B90-10
25	−3	70	30	B70-30
17	7	90	10	B90-10

Table 2. Cont.

Main Injection Timing (°C)	Post-Injection Timing (°C)	Main Injection Quantity (%)	Post-Injection Quantity (%)	Fuel Proportion
21	0	80	20	D80-20
25	7	90	10	B90-10
25	−7	90	10	D90-10
19	3	80	20	B80-20
25	7	70	30	B70-30
21	3	80	20	B80-20
17	−7	70	30	B70-30
23	7	70	30	B70-30
21	−7	80	20	B80-20
25	−3	90	10	D90-10
23	0	80	20	D80-20
21	3	80	20	B80-20
17	−7	70	30	B70-30
25	−7	70	30	B70-30
21	0	80	20	D80-20
23	−7	90	10	B90-10
19	−3	80	20	B80-20
17	7	90	10	D90-10
17	−7	70	30	B70-30
21	−3	80	20	D80-20
17	−3	90	10	B90-10
21	0	80	20	B80-20
19	3	90	10	B90-10
17	7	70	30	B70-10
17	−7	90	10	B90-10
19	0	80	20	D80-20
19	−7	80	20	B80-20
23	−7	90	10	D90-10

#### 2.4. Prediction of Diesel Engine Emissions and Combustion Characteristics Using ANN

The Bayesian neural network strategy is a sophisticated approach that serves as an effective means for improving the generalization capabilities of neural networks. This technique incorporates the Bayesian framework, which introduces modifications to the performance function that deviate from the conventional sum of squares of the network errors on the training set. The network weights and biases are considered random variables within this framework, with predetermined distributions. The unknown variance that is associated with these distributions is linked to regularization parameters, thereby improving the performance and precision of the network [16]. Statistical methods can be used to estimate these parameters. The mean sum of squared network errors serves as the objective function in the BRNN. A linear combination of weights and squared errors is minimized by BRNN [19]. Additionally, it changes the linear combination so that the final network has high generalization capacities. Training is terminated when any of the following conditions are met: the maximum number of epochs is reached, the maximum time limit is exceeded, or the performance has reached its goal. Additionally, training is halted if the performance gradient falls below the minimum gradient or if the learning momentum exceeds the specified maximum range. In MATLAB, any type of network, including artificial neural networks (ANN), can be trained using the “trainbr” command, provided that the network’s weight, net input, and transfer functions contain derivative functions [20,21]. Hence, in this present work, BRNN associated with the logistic–sigmoid transfer function was used to predict the engine characteristics; the input variables for ANN modeling were main injection timing ( $X_1$ , 17–25 °C), post-injection timing ( $X_2$ , 7 °C bTDC–7 °C aTDC), main injection quantity ( $X_3$ , 70–90%), and post-injection fuel quantity ( $X_4$ , 10–30%). Fuel proportion ( $X_5$ , diesel and biodiesel) and BTE, CO, UBHC, NO, smoke,

CGPP, and HRR were output responses. The architecture of the artificial neural network (ANN) model for the diesel engine characteristics is illustrated in Figure 2.

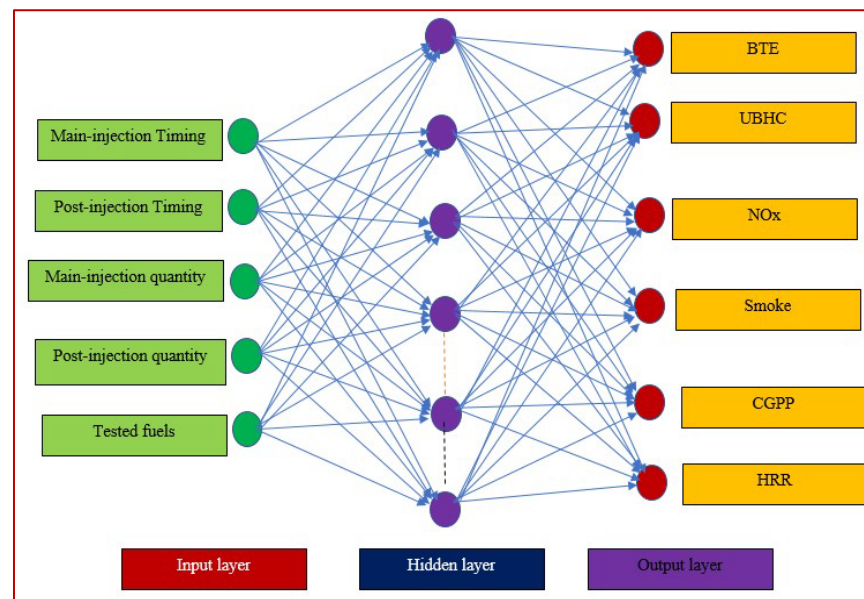


**Figure 2.** ANN architecture for the diesel engine characteristics model.

### 2.5. Experimental Setup and Uncertainty Analysis of Engine Study

An experimental study was carried out at the Sri Venkateswara Engine Testing Laboratory in Chennai, India, to analyze the impact of split injection techniques on the characteristics of a diesel engine when using blends of mixed waste cooking oil biodiesel and diesel fuel (Figure 3). The engine was operated at an optimal fuel injection pressure of 500 bar. The experiment involved the modification of the main injection timing from 17 to 25 °C and the post-injection timing from 7 bTDC to 7 aTDC. Additionally, the experiment involved varying the fuel injection levels, which included different proportions of main- and post-injection fuel quantities, namely 70–30%, 80–20%, and 90–10%. The diesel engine performance, emissions, and combustion characteristics were recorded at 100% engine load. Further, the study measured the exhaust emissions, specifically UBHC, NO, and smoke, using a five-gas analyzer and smoke meter equipped with NDIR and FID detectors.



**Figure 3.** Photographic view of the engine experimental setup.

## 3. Results and Discussion

### 3.1. Bio-Catalyst Characterization

#### X-ray Diffraction Analysis for Bio-Catalyst

An Ultima III diffractometer was used to record the bio-catalyst's X-ray diffraction pattern (Rigaku, Tokyo, Japan). The bio-catalyst's wide-angle X-ray diffraction pattern is

displayed in Figure 4. The (0 0 3) plane is the distinctive graphitic structural peak found at 21.19°. The  $K_2CO_3$ , KCl, and  $K_2SO_4$  reflections are the main visible in the prepared bio-catalyst. The face-centered crystal structure of  $K_2CO_3$  has peaks at 25.7°, 29.6°, 32.1°, 32.3°, and 32.6°, which correspond to the (0 0 4), (0 4 1), and (3 3 0) planes. The detection of peaks at 29.9° and 30.4° corresponding to the (1 3 0) and (2 2 0) planes, respectively, allowed for the identification of the face-centered crystal structure of  $K_2SO_4$ . A second peak at 28.28° reveals the KCl reflection plane (2 2 0). The Debye–Scherrer formula was used to determine the average catalyst’s crystalline size, which was found to be 56.66 nm.

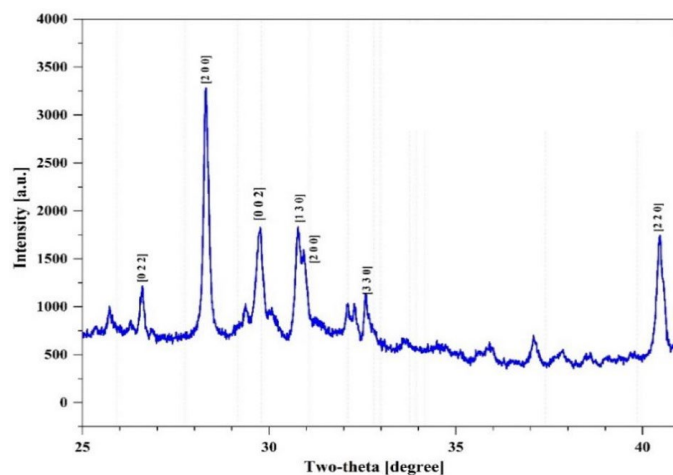


**Figure 4.** X-ray diffraction pattern for bio-catalyst synthesized from vegetable wastes.

### 3.2. Biodiesel Process Optimization Using the RSM Approach

Multiple regression analysis was performed on the results from the CCD experimental design (Table 1), and it was determined that the quadratic regression model is the best to forecast the process parameters in biodiesel production from MWCO using bio-catalyst. The positive and negative signs denote a synergistic impact and an antagonistic effect. An ANOVA table was employed to evaluate the significance and relevance of the quadratic model and the influence of all factors on the biodiesel synthesis process, and an ANOVA table was employed. In statistical analysis, a model term is considered significant if its *p*-value is less than 0.05, and a value above 1.000 indicates its importance. Additionally, the lack of fit F-value of 2.35 (>F-Table) suggests that the model adequately describes the variations in the response variable. The  $R^2$  value in this study was 98.45%, and the adjusted  $R^2$  value was 95.45%, whereas the predicted  $R^2$  value was 96.4%. The adjusted  $R^2$  is used to remove the undesired effects since it shows how well the model fits experimental data as well as anticipated data. The quadratic model has satisfactory agreement since the variation between forecasted and adjusted is less than 0.2. The point prediction methodology was employed to optimize the parameters involved in biodiesel production. According to the optimization results, the optimal parameters produced a biodiesel yield of 91.4% with a catalyst loading of 6.8 wt.%, 1:8.5 molar ratio, 55 °C temperature, 850 rpm, and 115 min of reaction time. Finally, the best combination was experimentally tested three times to validate the optimal conditions. The dissimilarity between the projected and experimental values is 1.6%, which indicates that the suggested model was accurately computed and the circumstances were optimal for biodiesel synthesis.

$$Y = +88.64 + 0.66A \pm 3.35B + 3.57C - 4.56D - 2.40E - 0.074AC + 2.18AD + 0.93BC - 2.04BD + 2.13BE - 0.59CD - 1.03CE - 1.12DE + 2.01A^2 - 1.07B^2 - 3.46C^2 - 4.91D^2 - 8.70E^2 \quad (1)$$

The 3D surface plot in Figure 5 exhibits the collective impact of catalyst concentration and molar ratio on biodiesel production while keeping other variables at their default values. The investigation revealed that biodiesel yield increased as the catalyst concentration was raised from 1 to 9 wt.%, and the molar ratio was elevated from 1:3 to 1:12.

Furthermore, it was demonstrated that elevating the concentration from 5 to 7 wt.% caused a significant increase in biodiesel yield, whereas increasing the catalyst loading from 7 to 9 wt.% had a minor negative impact on the yield. The performance and catalyst activity of the catalysts are impacted by the catalyst loading, which is a crucial element impacting biodiesel production. The proper catalyst concentration not only boosts the biodiesel yield but also stops unwanted side effects such as saponification and hydrolysis reactions [22,23]. Additionally, the decrease in biodiesel yield may be a slower mass transfer rate [14]. Further, an increase in the catalyst quantity increased the viscosity of the mixture, resulting in lower biodiesel yield. Increasing the catalyst loading in the biodiesel production from 5 to 7 wt.% is economically viable, and the optimum catalyst loading is 7 wt.%.

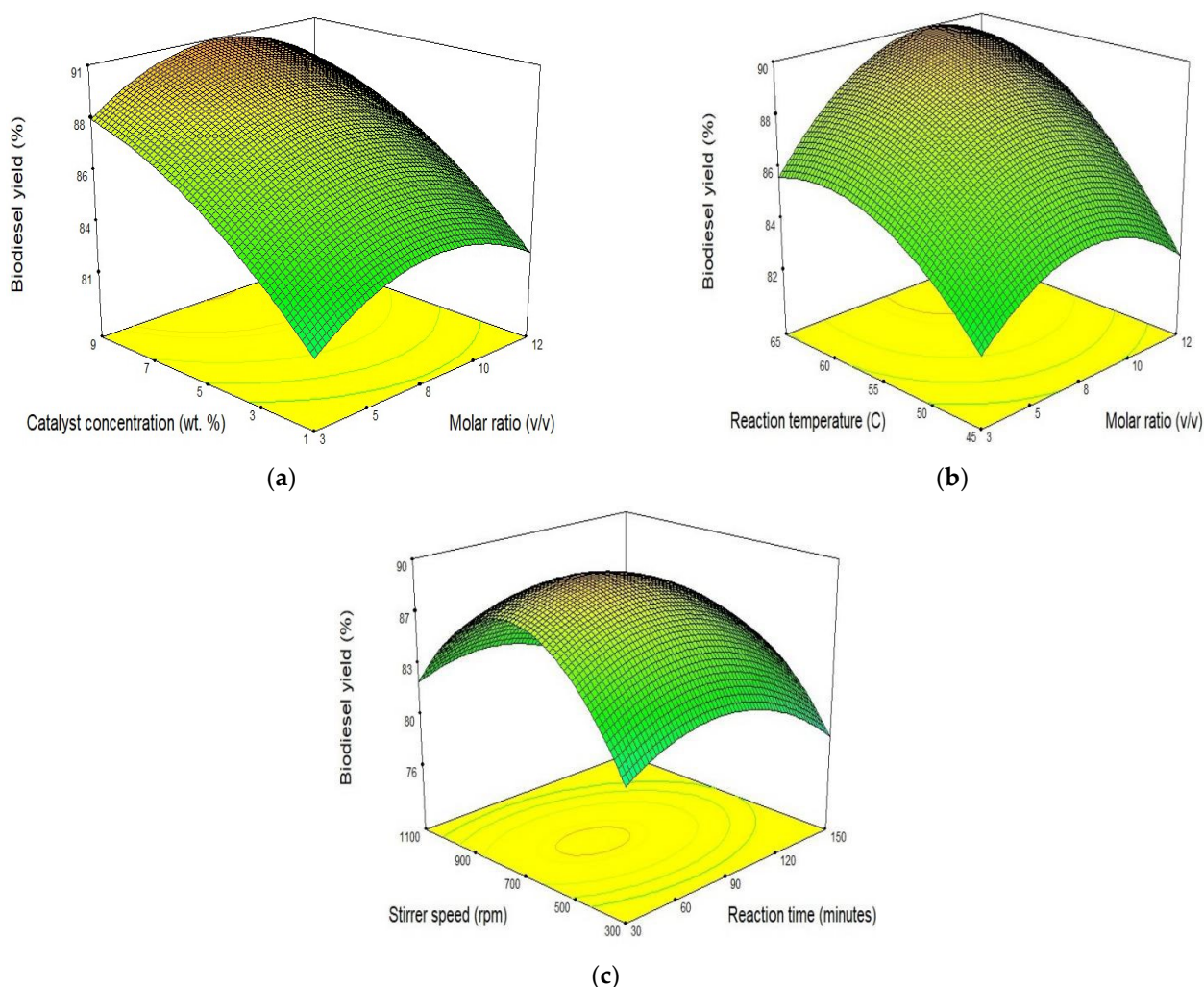


**Figure 5.** Three-dimensional plot of biodiesel yield as a function of (a) catalyst concentration vs. molar ratio, (b) reaction temperature vs. molar ratio, and (c) stirrer speed vs. reaction time.

Despite the stoichiometric molar ratio of methanol to oil for the transesterification process being 1:3, typically, the conventional practice for mechanical agitation homogeneous catalyst systems is to employ a 1:6 molar ratio. This is due to decreased catalyst activity and a slow reaction rate. Figure 5b shows the response surface plot of the biodiesel yield, while other parameters such as stirrer speed, catalyst loading, and time are remaining constant. As seen in Figure 5b, raising the molar ratio initially boost the biodiesel yield at a constant time and speed. The yield of the reaction remains largely unaffected by adding more methanol to the reaction mixture, although increasing the methanol ratio has a detrimental effect on the yield of biodiesel. Moreover, increasing the methanol-to-oil molar ratio from 1:9 to 1:15 does not expedite the process. Further, an upsurge in the molar

ratio above 1:9 was observed to lower the biodiesel yield. This conclusion was further supported by the interaction term ( $-0.074$ ) on the regression model equation connected to the molar ratio and temperature. A rise in the methanol-to-oil ratio causes a reversible transesterification reaction [24]. However, the following factors may be the causes for the drop in biodiesel yields such as higher polarity, glycerin solubility, and interference with glycerin [25]. As shown in Figure 5a,c, reaction duration (60–120 min) increases the biodiesel yield at constant catalyst concentration; a longer reaction time and an increasing the stirrer speed resulted in a significant drop in biodiesel yield. Longer reaction time at higher speed results in a more intense emulsion of biodiesel, glycerol, and methanol, which reduces the biodiesel yield by slowing separation and purification. Further, longer reaction time and high stirrer speed result in increased viscosity and foam formation, which also lead the reaction to develop in an unfavorable direction [14].

### 3.3. Optimization of Diesel Engine Combustion and Emissions Characteristics using the RSM Method

Figure 6 illustrates a comparison between brake thermal efficiency (BTE) and different injection timings and fuel quantities. According to the experimental studies, B100-90%-10% with a main injection timing (MIT) of  $25^{\circ}\text{C}$  bTDC and post-injection timing of  $7^{\circ}\text{C}$  bTDC achieved the maximum brake thermal efficiency (BTE) of 34.23%. This value is 1% less than that for conventional diesel under the same operating conditions. At an optimum main injection timing (MIT) of  $25^{\circ}\text{C}$  and post-injection timing of  $7^{\circ}\text{C}$  bTDC, the CCD and ANN methods predicted a maximum brake thermal efficiency (BTE) of 33.25% and 34%, respectively. However, there was a slight deviation of 1% and 0.23%, respectively, between these predicted values and the experimental results. Thus, the experimental results are in excellent accordance with the projected outcomes from both RSM and ANN. It was discovered that advancing the MIT and PIT timing could boost the engine performance for biodiesel and conventional diesel [15]. However, the engine BTE was decreased when the MIT and PIT injection timing was retarded and post-injection quantity minimized. This is due to delayed injection results in partial combustion due to a shorter ignition delay period [14]. Additionally, it can be seen that the minimum quantity of post-injection increased the engine BTE. This is because post-injection enables higher utilization as compared to a single injection strategy. The fuel blend containing B100-70%-30% yielded the lowest BTE of 30% at  $17^{\circ}\text{CA}$  bTDC and  $7^{\circ}\text{CA}$  aTDC, and this was consistent with the findings for both the RSM and ANN methods. The remaining combinations exhibited inferior performance compared to B100-90%-10%. Furthermore, due to the high oxygen content in biodiesel, the combustion process is enhanced, and the controlled combustion process is further improved with a small amount of post-injection, leading to improved engine performance.

A comparison between UBHC emissions of biodiesel under different fuel injection quantities and injection timings is depicted in Figure 7a,b. As depicted in Figure 7a, an increase in the percentage of main injection fuel quantity from 70% to 90% results in a corresponding increase in UBHC emissions. However, Figure 7b shows that as the injection timing is advanced from  $17^{\circ}\text{C}$  and  $7^{\circ}\text{C}$  bTDC to  $7^{\circ}\text{C}$  bTDC, UBHC emissions decrease. The existence of UBHC in the exhaust gas indicates the incomplete combustion of fuel. B100-80%-20% emits the least UBHC, 14 ppm, when compared to other combinations such as B100-70%-30% and B100-90%-10% and conventional diesel. The results suggest that advancing the injection timing leads to lower UBHC emissions, regardless of the injection quantity. It progresses the spray characteristics, which aid in complete combustion [26]. Further, RSM determined the maximum UBHC, 17 ppm, for B100-90%-10% at  $17^{\circ}\text{C}$ , which is comparable to the experimental results and demonstrates zero error in the RSM prediction and ANN method. Around 26% UBHC emission reduction was observed when 80%-20% of fuel was injected as main and post-injection fuel at MIT of  $25^{\circ}\text{C}$  and PIT of 7 bTDC at an injection pressure of 500 bar. This can be attributed to the fact that early injection and higher injection pressure create smaller fuel droplets, which enhance the fuel-air mixing process

and reduces the formation of fuel-rich regions, resulting in lower UBHC emissions [26]. Additionally, the occurrence of oxygen in biodiesel stimulates the oxidation of UBHC and minimizes the formation of UBHC emissions.

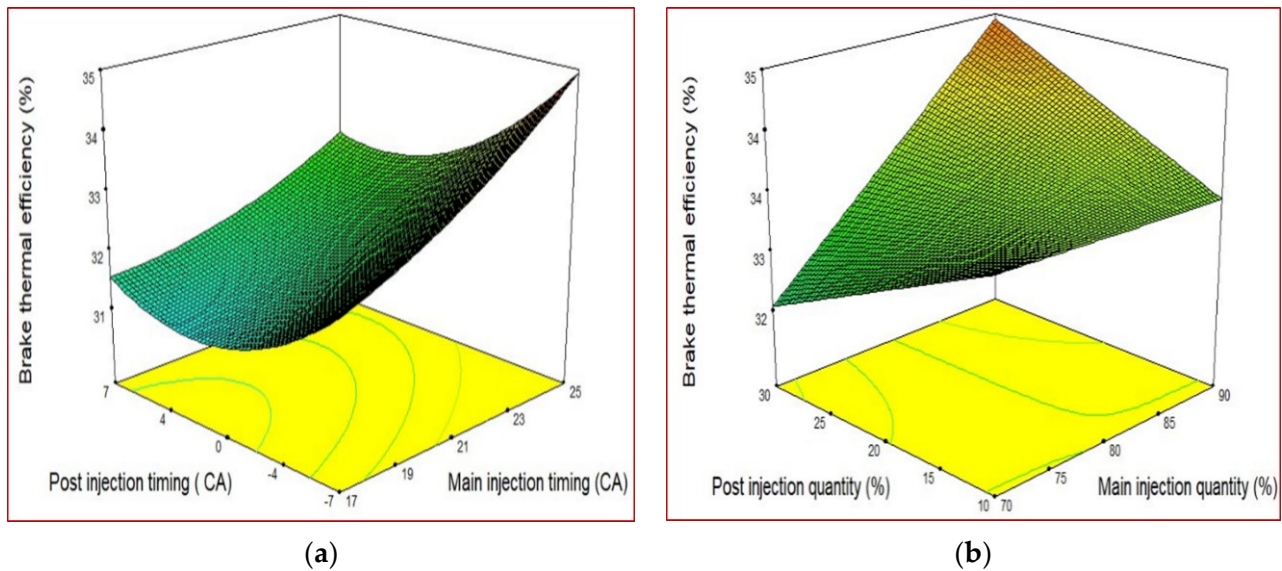


**Figure 6.** Variation in (a) brake thermal efficiency with respect to main injection and post-injection timing, and (b) main- and post-injection fuel quantity.

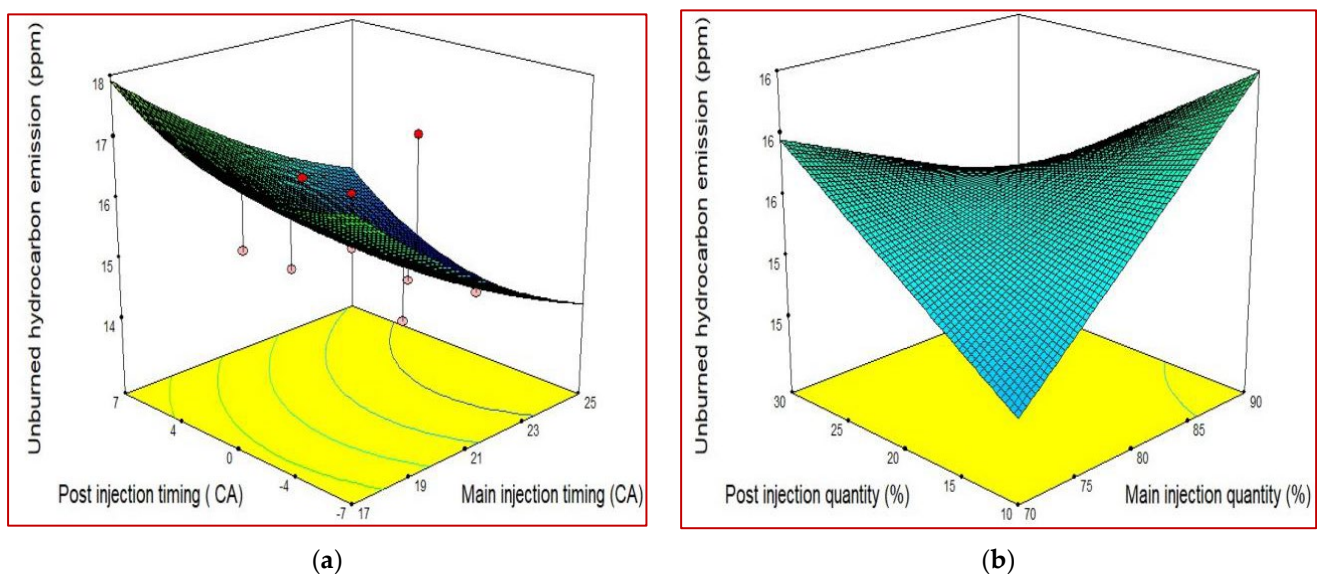


**Figure 7.** Comparison of unburned hydrocarbon emission of (a) main injection and post-injection timing, and (b) main- and post-injection fuel quantity.

The 3D plot shown in Figure 8a,b compares the nitric oxide (NO) emission of biodiesel and diesel in relation to the fuel injection quantities and timing of main- and post-injection. The results indicate that an increase in the main injection fuel quantity from 75% to 90%, as shown in Figure 8b, leads to an increase in NO emission. The experimental findings indicate that the maximum NO emissions of 1310 and 1233 ppm, respectively, were attained for B90%-10% and B80%-20%. The increase in nitric oxide emissions with higher main injection fuel quantities, as observed in Figure 8b, is caused by higher pressure and temperature in the combustion chamber, together with longer residence times that promote the formation of nitric oxide [27]. Further, increase in premixed combustion and NO emission formation

are caused by higher dwell time and proportion of main injection fuel quantity. Figure 2a indicates that an increase in NO emission formation occurred when the main injection timing was increased from 17 to 25 °C and the fuel quantity was increased from 70% to 90%. The delayed fuel injection timing in B80%-20% and B70%-30% led to reduced in-cylinder pressure, resulting in lower in-cylinder temperature and, ultimately, minimum NO emissions of 878 and 869 ppm, respectively, at a post-injection timing of 7 °C aTDC. As the main injection timing is retarded, the NO emission consistently decreases. The primary reason is that it lowers the temperature at which fuel is burned inside the cylinder, as well as the amount of time high-temperature burned gas is allowed to remain in the combustion chamber [28].

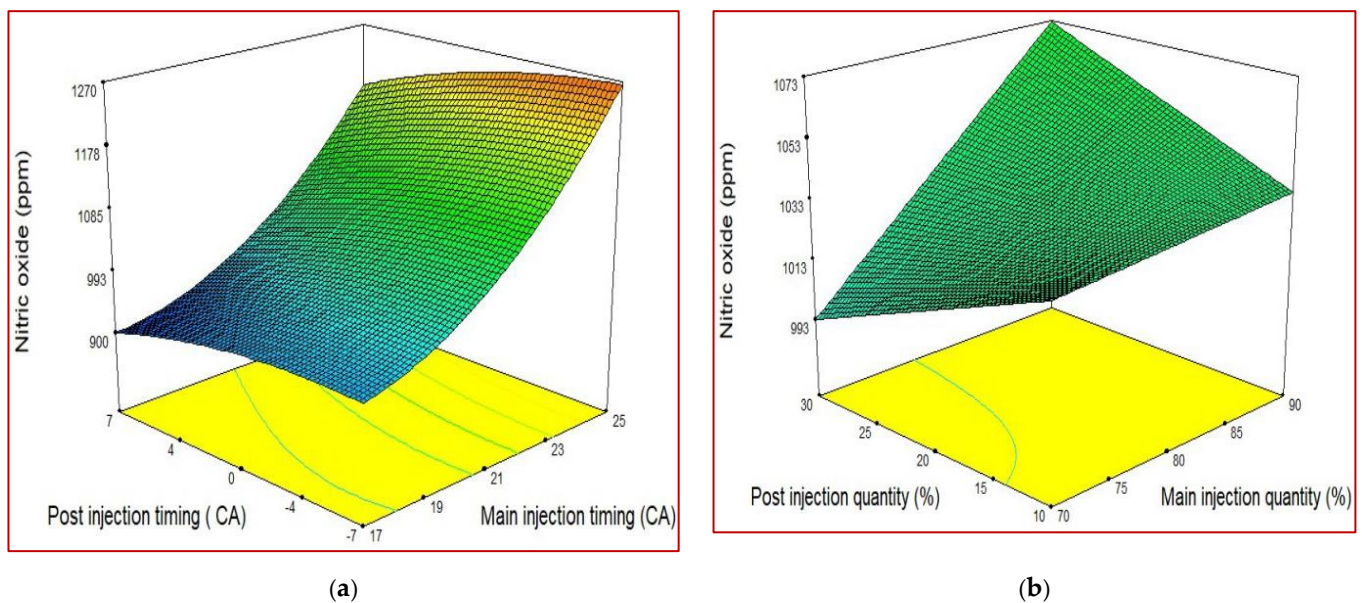


**Figure 8.** Nitric oxide emission from biodiesel fuel engine under effects of (a) post-injection timing vs. main injection timing and (b) post-injection quantity vs. main injection quantity.

Figure 9a,b compare smoke emissions for different biodiesel proportions under varying main injection and post-injection timing. Experimental findings show that advanced injection timing for B100-80%-20% lowers the smoke emission while retarded injection timing at 17 °C increases the smoke emission. Advanced timing led to an improvement in smoke emission as it provided more time for the air–fuel mixture to be prepared appropriately, resulting in reduced emissions. The extended ignition delay period and increased injection pressure improved droplet evaporation and combustion, resulting in an enhanced combustion process. Further, biodiesel burns more completely and produces lesser exhaust emissions because of the high oxygen content compared to diesel [9]. The utilization of B100-80%-20% fuel, along with an MIT of 25 °C and PIT of 6 °C bTDC, resulted in the lowest exhaust emission, 1.653 FSN. This outcome can be attributed to the post-injection quantity, which improves controlled combustion by facilitating proper evaporation and eliminating fuel-rich zones, ultimately reducing smoke emission formation. The RSM projected value is 0.312 FSN lower than the experimental value; therefore, RSM is strongly advised for predicting diesel engine characteristics. However, B100-90%-10% obtained the highest smoke emission, 2.675 FSN, at MIT of 17 °C and PIT of 7 °C aTDC. A comparable smoke emission of 2.673 was discovered for B100-90%-10% using the RSM approach higher injection pressure results in fine fuel droplets and more surface area, which improves fuel and air mixing.

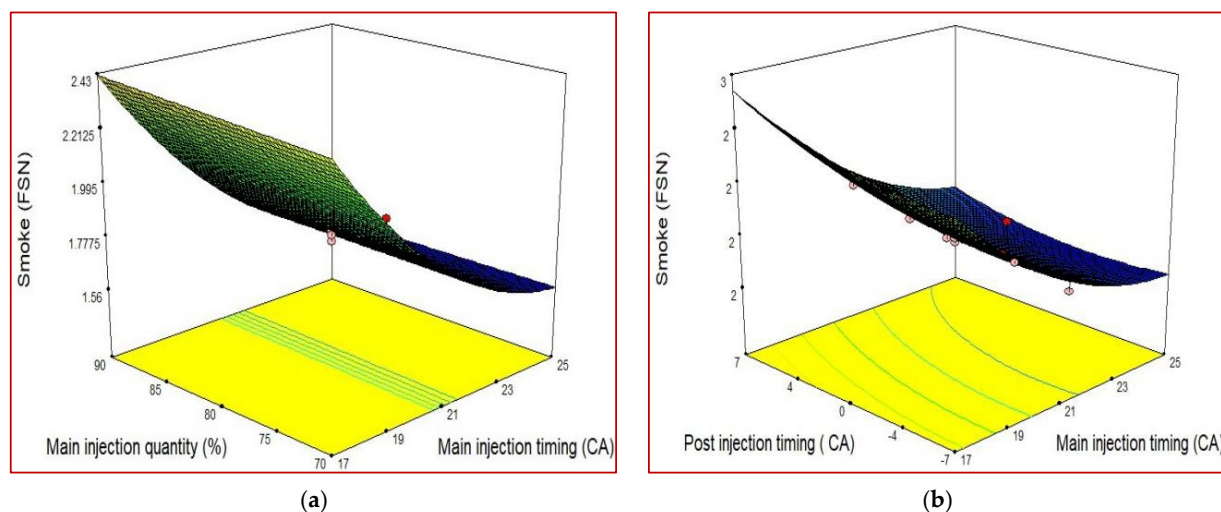


**Figure 9.** Variation in smoke emission from biodiesel fuel engine under different (a) main injection timing vs. main injection quantity and (b) post-injection timing vs. main injection timing.

Figure 10 demonstrates the relationship between cylinder peak pressure (CPP) and injection timing, injection quantity, and fixed injection pressure. An increase in CPP is an indication of improved combustion quality [29]. Increasing the primary fuel injection amount led to greater premixed combustion, resulting in an elevation of the CGPP. The finding demonstrates that the physical characteristics of biodiesel lead to lower CGPP. Enhanced combustion achieved through a combination of advanced injection timing and increased primary fuel injection quantity resulted in an elevation of the CGPP. The proper fuel–air mixture produces better premixed combustion than controlled combustion, which leads to higher CGPP. The main injection quantity and advanced MIT and PIT timing produced the highest CGPP. The RSM forecast indicated that D100-90%-10%, B100-80%-20%, and B100-70%-30% fuels exhibited the highest CGPP at 64 bar, 63 bar, and 100% load, respectively. The strong correlation between the RSM-predicted values and the actual experimental results underscores the efficacy of RSM as a reliable method for forecasting diesel engine characteristics. B100-80%-20% and B100-70%-30% attained minimum CGPP at retarded injection timing and minimum fuel injection quantity was discovered from the RSM prediction, which was in good agreement with the experimental findings. Owing to main injection timing being delayed, poor vaporization and lower CGPP resulted. Rapid injection pressure increases not only result in reduced fuel economy and engine vibrations but also have an impact on NO emission [9]. Employing split injection instead of a single injection led to a reduction in peak pressure and an extension of the p-curve. In single injection mode at 500 bar, the maximum pressure was recorded as 72 bar [14]. However, introducing the main injection at 25 °C with the same injection pressure resulted in a reduced peak pressure of 64 bar.

Figure 11 depicts the heat release rate at maximum load for both conventional diesel and biodiesel. The evaporation of the mixture is indicated by the negative slope of the tested fuels, followed by the appearance of two positive curves for premixed and controlled combustion. According to Figure 11a, the HRR of biodiesel increased when MIT and PIT timing advanced. At an MIT of 25 °C and a PIT of 7 °C bTDC, B100-90%-10% fuel exhibited an HRR of 53 J/°C, while diesel had a maximum HRR of 55 J/°C. Biodiesel exhibits a consistently lower heat release rate (HRR) compared to diesel, irrespective of the injection pressure, timing, or fuel quantity, owing to its lower burning velocity, higher viscosity, and lower volatility [14]. Advanced MIT and PIT timing resulted in the highest HRR due to a prolonged delay that led to increased evaporation rate and improved air–fuel mixture process. When the injection was done in accordance with the experimental conditions with split injection, two HRR trends were seen. The maximum heat emitted during premixed combustion increased the HRR for the tested fuel at advance timing and higher main

injection fuel quantity. The rapid evaporation of the fuel during the main injection and subsequent combustion results in a reduced physical delay of the fuel, leading to an overall increase in the HRR rate. The polynomial equations for the RSM model follow:

$$Y_{bte} = +31.69 + 0.7 - 8.90C^2 + 5.32AD^2 - 0.43E^27A - 0.55B + 0.42C - 0.24AC + 0.034BC + 0.47CD + 1.04A^2 - 0.31B^2 \quad (2)$$

$$Y_{ubhc} = +15.09 - 1.50A + 0.41B + 0.40C - 0.06AB + 0.28AC + 0.42BC - 0.36CD + 0.25A^2 + 0.68B^2 \quad (3)$$

$$Y_{NO} = +1032.82 + 148.41A - 35.43B + 21.41C - 10.0AB + 12.80AC - 1.02BC + 18.35CD + 6.54A^2 - 19.44B^2 \quad (4)$$

$$Y_{smoke} = +1.80 - 0.41A + 0.10B + 0.015C - 0.046AB - 0.07AC - 0.040BC - 0.05CD + 0.18A^2 + 0.071B^2 \quad (5)$$

$$Y_{cgpp} = +63.08 + 1.02A - 0.26B - 0.14C - 0.336AB + 0.46AC - 0.26BC - 0.25CD + 0.20A^2 + 0.082B^2 \quad (6)$$

$$Y_{hrr} = +52.71 + 1.09A - 0.74B - 0.37C - 0.17AB - 0.054AC - 0.150BC - 0.70CD - 1.04A^2 + 0.131B^2 \quad (7)$$

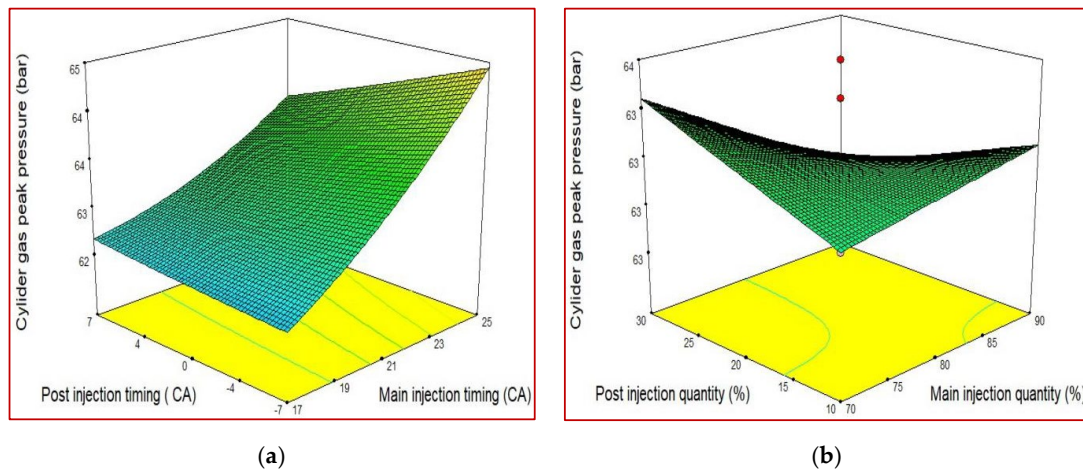


**Figure 10.** Effect on in-cylinder peak pressure of diesel engine characteristics under different (a) post-injection timing vs. main injection timing and (b) post-injection quantity vs. main injection quantity.

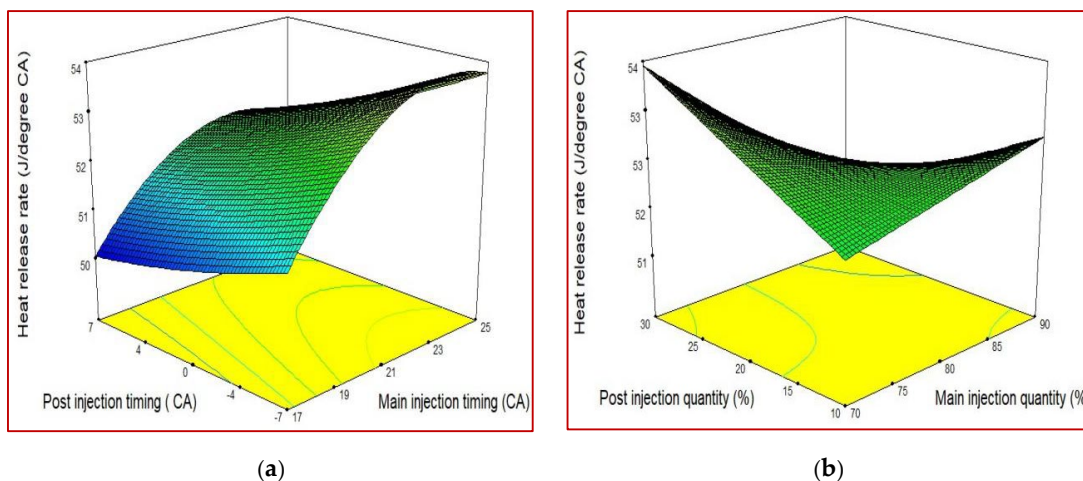


**Figure 11.** Influence of (a) post-injection timing vs. main injection timing and (b) post-injection quantity vs. main injection quantity on heat release rate of diesel engine emission during fuel testing.

### 3.4. Diesel Engine Performance and Combustion Characteristics Prediction Using ANN

Figure 12 illustrates the variation in the number of neurons utilized in diesel engine modeling, as determined through evaluation of the mean square error (MSE) and  $R^2$  values. The superiority of neural networks over linear transformations is due to the nonlinearity of their transfer function. Topological research employed MSE as the performance criterion, with the number of neurons varying between 12 and 26 for each iteration. The neural network was constructed and trained using data from Table 2, which encompassed a total of 32 data points. Out of these, 15% were reserved for testing, 15% for validating the ANN model, and 70% for training. The input and output values were normalized prior to training to avoid over-fitting issues. Upon reaching a low MSE value, network training was terminated, which required nine iterations (epochs) to achieve. It can be seen that all prediction networks exhibit extremely good  $R^2$  values (0.911, 0.945, 0.99, and 0.997, respectively). These results indicate that ANN produces highly accurate results in modeling engine combustion, emission, and performance characteristics. Excellent compatibility between test results and ANN results, all of the data are dispersed over the 45° line. The values of  $R^2$  between the test and ANN projected outcomes clearly show that the ANN model was accurate in estimating the engine performance and emissions such as UBHC, NO and smoke, followed by combustion characteristics such as CGPP and HRR.

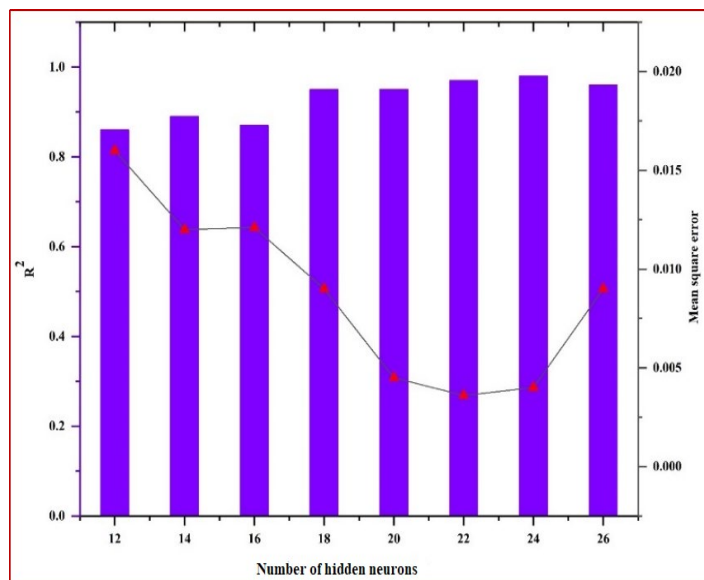


**Figure 12.** Selection of neurons for ANN modeling based on MSE (Red triangle) and  $R^2$  values.

### 3.5. Comparison between RSM and ANN Technique

Figure 13 depicts the relationship between experimental results and the estimations made by ANN and RSM. It can be seen that ANN estimation and experimental values agree more closely than RSM estimation. The best fit is obtained with BTE, NO, and smoke emissions, followed by UBHC, CGPP, and HRR when the ANN model estimations are taken into account. According to estimates from the RSM model, NO and smoke emissions are the best responses that match experimental data. The highest BTE, 33.25% and 34%, was forecasted by the CCD and ANN methods, respectively, at an MIT of 25 ° CA, and timing of 7 °C bTDC, which is 1 % and 0.23%, respectively, deviated from the experimental results. The ANN and RSM methods accurately predicted the minimum UBHC emissions, with both methods yielding results of 14 and 15 ppm, respectively, which aligned with the experimental data. Similarly, the ANN and RSM methods projected a minimum NO emission of 889 and 921 ppm, respectively, which closely approached the experimental values. The performance and modeling capabilities of the RSM appear to be not very strong when compared to the ANN model, which has  $R^2$  values between 0.88 and 0.95, and the proposed ANN model that has  $R^2$  values over 0.98. Concerning

performance, the ANN model performed well as compared to the RSM model. It was noticed that the ANN demonstrated a definite superiority over RSM in terms of modeling and optimization methodologies.

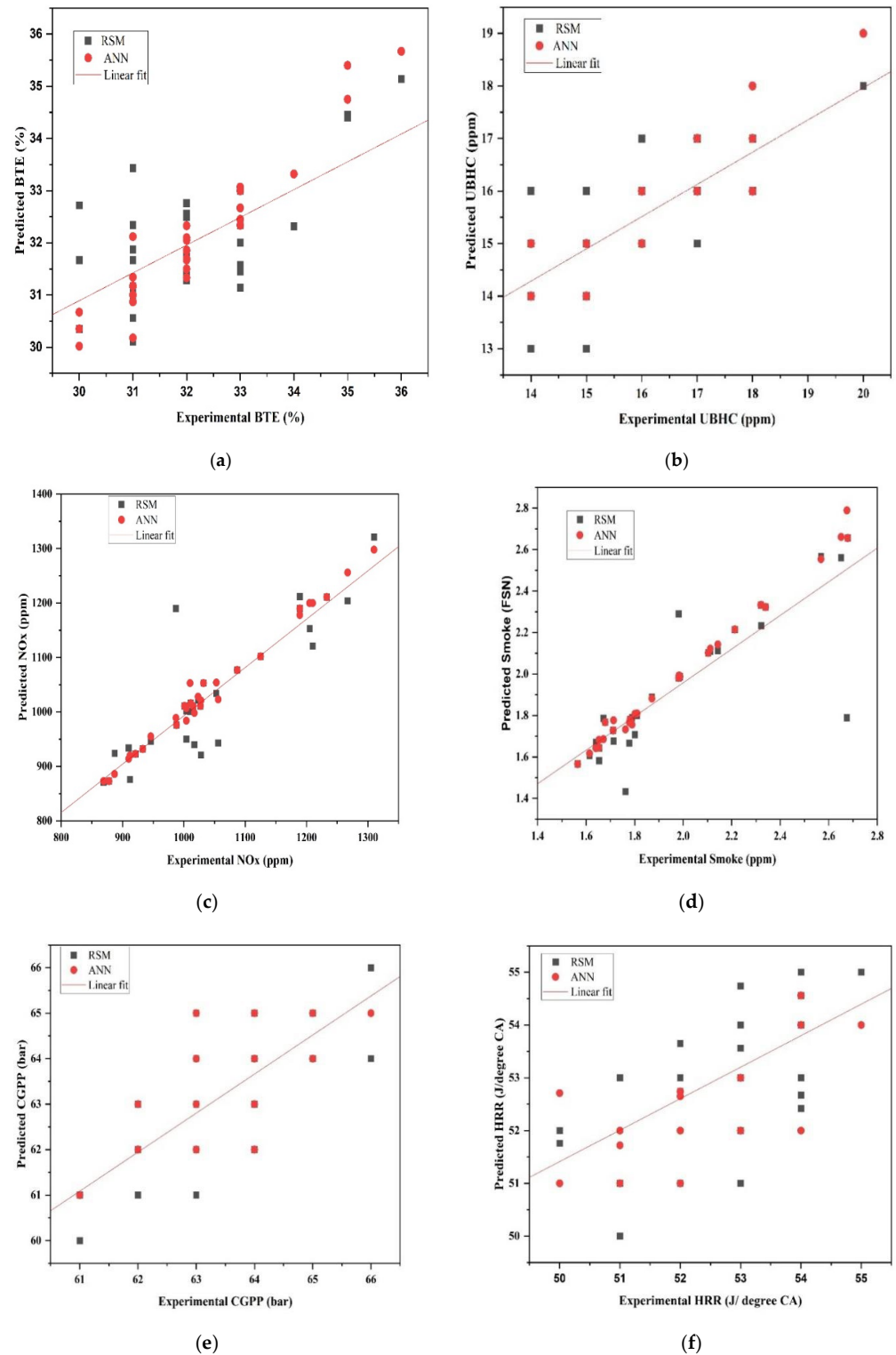


**Figure 13.** Comparison of experimental results with predicted ANN and RSM results: (a) BTE, (b) UBHC, (c) NO<sub>x</sub>, (d) smoke emission, (e) CGPP, and (f) HRR. Black dot and red dot/red square represent the predicted RSM and ANN values, respectively.

#### 4. Conclusions

The experimental study aimed to assess the impact of main injection and post-injection timing, along with fuel injection quantity, on the characteristics of a CRDI-assisted diesel engine running at 100% load. The biodiesel was synthesized from MWCO using a bio-catalyst derived from vegetable wastes as a catalyst. In this research, the combustion and emissions characteristics of an engine were optimized using RSM and ANN methods, and the results obtained were validated by comparing them with experimental data. According to the RSM analysis, a catalyst loading of 6.8 weight percent, a molar ratio of 1:8.5, a reaction temperature of 55 °C, and a stirrer speed of 850 rpm could be used to produce the best biodiesel yield of 94%. The findings of this study could potentially be useful in developing more efficient and sustainable biodiesel production processes. It was discovered that variations in fuel injection quantity and injection timing under a higher injection pressure of 500 bar had a significant impact on UBHC, NO, and smoke emissions, in addition to performance merits such as BTE, CGPP, and HRR. The split injection technique significantly reduced the peak pressure due to early heat release caused by the main injection and delay in post-injection. In comparison to the single injection mode, the brake thermal efficiency (BTE) decreased by 2% at the same injection pressure and timing. Furthermore, the split injection strategy resulted in a maximum reduction of 30% in NO emissions, observed at 17 °C and 7 °C aTDC at a pressure of 500 bar when compared to the single injection strategy mode. These findings suggest that the split injection technique could be a viable solution to improve engine performance and reduce NO emissions in diesel engines. Based on the study's findings, the split injection strategy, which involves a delayed injection timing and increased post-injection quantity, effectively reduces NO emissions while producing lower levels of UBHC and smoke emissions without compromising engine efficiency compared to the single injection strategy. Future studies could advance the understanding of the impact of fuel composition and operating factors on combustion and emissions characteristics by investigating the use of MWCO biodiesel–diesel blends in conjunction with the split injection strategy and EGR technique. Such research would provide valuable insights into the potential benefits of split injection and contribute to the development of cleaner and more efficient diesel engine technologies.

**Author Contributions:** Conceptualization, B.D., S.A. (Santhoshkumar Annamalai), and M.S.; methodology, B.D. and S.A. (Santhoshkumar Annamalai); validation, B.D. and S.A. (Santhoshkumar Annamalai); formal analysis, B.D. and S.A. (Santhoshkumar Annamalai); investigation, B.D. and S.A. (Sukunya Areeya); data curation, B.D. and K.R.; writing—original draft preparation, B.D. and S.A. (Santhoshkumar Annamalai); writing—review and editing, B.D., K.R., K.K., P.-L.S. and M.S.; supervision, M.S.; project administration, M.S.; funding acquisition, M.S. All authors have read and agreed to the published version of the manuscript.

**Funding:** This research was funded by King Mongkut's University of Technology North Bangkok, grant number KMUTNB-66-BASIC-16 and KMUTNB-Post-65-09.

**Data Availability Statement:** Data available on request due to restrictions.

**Acknowledgments:** The authors grateful to the King Mongkut's University of Technology North Bangkok (Grant No. KMUTNB-66-BASCI-16 and KMUTNB-Post-65-09) for financial assistance.

**Conflicts of Interest:** The authors declare no conflict of interest.

#### References

1. Teoh, Y.H.; How, H.G.; Lee, S.W.; Loo, D.L.; Le, T.D.; Nguyen, H.T.; Sher, F. Optimization of engine out responses with different biodiesel fuel blends for energy transition. *Fuel* **2022**, *318*, 123706. [[CrossRef](#)]
2. Gundupalli, M.P.; Sriariyanun, M. Recent Trends and Updates for Chemical Pretreatment of Lignocellulosic Biomass. *Appl. Sci. Eng. Prog.* **2023**, *16*, 5842. [[CrossRef](#)]
3. Binhweel, F.; Hossain, M.S.; Ahmad, M.I. Recent Trends, Potentials, and Challenges of Biodiesel Production from Discarded Animal Fats: A Comprehensive Review. *BioEnergy Res.* **2022**. [[CrossRef](#)]

4. Mandari, V.; Devarai, S.K. Biodiesel Production Using Homogeneous, Heterogeneous, and Enzyme Catalysts via Transesterification and Esterification Reactions: A Critical Review. *BioEnergy Res.* **2022**, *15*, 935–961. [[CrossRef](#)]
5. Samanta, S.; Sahoo, R.R. Waste Cooking (Palm) Oil as an Economical Source of Biodiesel Production for Alternative Green Fuel and Efficient Lubricant. *BioEnergy Res.* **2021**, *14*, 163–174. [[CrossRef](#)]
6. Balajii, M.; Niju, S. A novel biobased heterogeneous catalyst derived from *Musa acuminata* peduncle for biodiesel production—Process optimization using central composite design. *Energy Convers. Manag.* **2019**, *189*, 118–131. [[CrossRef](#)]
7. Chuah, L.F.; Amin, M.M.; Yusup, S.; Loo, D.L.; Le, T.D.; Raman, N.A.; Bokhari, A.; Klemes, J.J.; Alnarabiji, M.S. Influence of green catalyst on transesterification process using ultrasonic-assisted. *J. Clean. Prod.* **2016**, *136*, 14–22. [[CrossRef](#)]
8. Yusuff, A.S.; Bhonsle, A.K.; Bangwal, D.P.; Atray, N. Development of a barium-modified zeolite catalyst for biodiesel production from waste frying oil: Process optimization by design of experiment. *Renew. Energy* **2021**, *177*, 1253–1264. [[CrossRef](#)]
9. Ramalingam, S.; Dhamalingam, B.; Deepakkumar, R.; Sriariyanun, M. Effect of *Moringa oleifera* biodiesel–diesel–carbon black water emulsion blends in diesel engine characteristics. *Energy Rep.* **2022**, *8*, 9598–9609. [[CrossRef](#)]
10. Dhamalingam, B.; Ramanathan, A. Biodiesel–diesel–alcohol blends as an alternative fuel for DIC engine. In *Advanced Biofuels: Applications, Technologies, and Environmental Sustainability*; Woodhead Publishing Series in Energy; Woodhead Publishing: Shaxton, UK, 2019; pp. 338–365.
11. Pavan, P.; Bhaskar, K.; Sekar, S. Effect of split injection and injection pressure on CRDI engine fuelled with POME–diesel blend. *Fuel* **2021**, *292*, 120242. [[CrossRef](#)]
12. Ravikumar, J.; Sekar, S.; Damodharan, D.; Yuvarajan, D.; Lakshmanan, T.; Mukilarasan, N.; Gopal, K.; Melvin, V.D.P. Multi-objective optimization of performance and emission characteristics of a CRDI diesel engine fueled with sapota methyl ester/diesel blends. *Energy* **2022**, *250*, 123709.
13. Ganesan, N.; Viswanathan, K.; Karthic, S.V.; Ekambaram, P.; Wu, W. Split injection strategies based RCCI combustion analysis with waste cooking oil biofuel and methanol in an open ECU assisted CRDI engine. *Fuel* **2022**, *319*, 123710. [[CrossRef](#)]
14. Dharma, B.; Karvembu, R.; Ramanathan, A. Impact of split injection strategy on combustion, performance and emissions characteristics of biodiesel fuelled common rail direct injection assisted diesel engine. *Energy* **2018**, *165*, 577–592.
15. Thangarasu, V.; Angkayarkan Vinayakaselvi, M.; Ramanathan, A. Artificial neural network approach for parametric investigation of biodiesel synthesis using biocatalyst and engine characteristics of diesel engine fuelled with Aegle Marmelos Correa biodiesel. *Energy* **2021**, *230*, 120738. [[CrossRef](#)]
16. Kumari, N.; Garg, S.; Singhal, A.; Kumar, M.; Bhattacharya, M.; Kumar Jha, P.; Kumar Chauhan, D.; Shekhar Thakur, I. Optimizing pretreatment of *Leucaena leucocephala* using artificial neural networks (ANNs), Bioresource. *Technol. Rep.* **2019**, *7*, 100289.
17. Tosun, E.; Aydin, K.; Bilgili, M. Comparison of linear regression and artificial neural network model of a diesel engine fueled with biodiesel–alcohol mixtures. *Alex. Eng. J.* **2016**, *55*, 3081–3089. [[CrossRef](#)]
18. Sriariyanun, M.; Kitiborwornkul, N.; Tantayotai, P.; Rattanaporn, K.; Show, P.L. One-Pot Ionic Liquid-Mediated Bioprocess for Pretreatment and Enzymatic Hydrolysis of Rice Straw with Ionic Liquid-Tolerance Bacterial Cellulase. *Bioengineering* **2022**, *9*, 17. [[CrossRef](#)]
19. Payal, A.; Rai, C.S.; Reddy, B.V. Comparative analysis of Bayesian regularization and Levenberg–Marquardt training algorithm for localization in a wireless sensor network. In Proceedings of the 2013 15th International Conference on Advanced Communications Technology (ICACT), PyeongChang, Republic of Korea, 27–30 January 2013.
20. Sivanandam, S.N.; Sumathi, S.; Deepa, S.N. *Introduction to Neural Networks Using Matlab 6.0 Computer Engineering Series*, 1st ed.; Tata McGraw-Hill: New Delhi, India, 2006.
21. Agrawal, T.; Gautam, R.; Agrawal, S.; Singh, V.; Kumar, M.; Kumar, S. Optimization of engine performance parameters and exhaust emissions in compression ignition engine fueled with biodiesel–alcohol blends using the taguchi method, multiple regression and artificial neural network. *Sustain. Futur.* **2020**, *2*, 100039. [[CrossRef](#)]
22. Eldiehy, K.S.H.; Gohain, M.; Daimary, N.; Borah, D.; Mandal, M.; Deka, D. Radish (*Raphanus sativus* L.) leaves: A novel source for a highly efficient heterogeneous base catalyst for biodiesel production using waste soybean cooking oil and *Scenedesmus obliquus* oil. *Renew. Energy* **2022**, *191*, 888–901. [[CrossRef](#)]
23. Siddavatam, N.K.R.; Mohmad, M.W. A Comprehensive Review on Effects of Nanoparticles–antioxidant Additives–biodiesel Blends on Performance and Emissions of Diesel Engine. *Appl. Sci. Eng. Prog.* **2020**, *13*, 285–298.
24. Mahesh, S.E.; Ramanathan, A.; Begum, M.S.; Narayanan, A. Biodiesel production from waste cooking oil using KBr impregnated CaO as catalyst. *Appl. Therm. Eng.* **2015**, *91*, 442–450. [[CrossRef](#)]
25. Yogesh, P.; Chandramohan, D. Combustion, performance and emissions characteristics of CRDI engine fueled with biodiesel, ethanol & butanol blends at various fuel injection strategies. *J. Appl. Sci. Eng.* **2022**, *25*, 1123–1129.
26. Jain, A.; Singh, A.P.; Agarwal, A.K. Effect of Split Fuel Injection and EGR on NO<sub>x</sub> and PM Emission Reduction in a Low Temperature Combustion (LTC) Mode Diesel Engine. *Energy* **2017**, *122*, 249–264. [[CrossRef](#)]
27. Park, S.; Kimb, H.J.; Shin, D.H.; Lee, J.T. Effects of various split injection strategies on combustion and emissions characteristics in a single-cylinder diesel engine. *Appl. Therm. Eng.* **2018**, *140*, 422–431. [[CrossRef](#)]

28. Dharmalingam, B.; Deepakkumar, R.; Bhattacharya, K.; Gundupalli, M.G.; Sriariyanun, M. Prediction of split injection strategy assisted diesel engine combustion, performance and emission characteristics fueled waste frying oil methyl ester through central composite design. *Mater. Today Proc.* **2023**, *72*, 2965–2970. [[CrossRef](#)]
29. da Silva, M.J.; de Oliveira, A.; Sodre, A.R. Analysis of processing methods for combustion pressure measurement in diesel engine. *J. Braz. Soc. Mech. Sci. Eng.* **2019**, *41*, 282. [[CrossRef](#)]

**Disclaimer/Publisher’s Note:** The statements, opinions and data contained in all publications are solely those of the individual author(s) and contributor(s) and not of MDPI and/or the editor(s). MDPI and/or the editor(s) disclaim responsibility for any injury to people or property resulting from any ideas, methods, instructions or products referred to in the content.